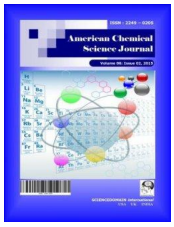

American Chemical Science Journal
9(1): 1-11, 2015, Article no.ACSJ.18766
ISSN: 2249-0205

SCIENCEDOMAIN *international*
www.sciencedomain.org

Nanocellulose Crystals from Coir Fibre for Template Application

E. U. Ikhuoria[1*], S. O. Omorogbe[2], O. G. Agbonlahor[1] and R. A. Etiuma[3]

[1]Department of Chemistry, University of Benin, Benin City, Nigeria.
[2]Materials Science and Technology Division, CSIR - National Institute for Interdisciplinary Science and Technology (NIIST), Thiruvananthapuram, Kerala - 695019, India.
[3]Department of Chemistry, University of Calabar, Calabar, Nigeria.

Authors' contributions

This work was carried out in collaboration between all authors. Authors EUI and SOO designed the study. Authors SOO and OGA performed the statistical analysis, wrote the protocol, and wrote the first draft of the manuscript. Authors EUI, SOO and RAE managed the analyses of the study. Authors OGA and RAE managed the literature searches. All authors read and approved the final manuscript.

Article Information

DOI: 10.9734/ACSJ/2015/18766
Editor(s):
(1) Gustaaf Schoukens, Department of Textiles, Ghent University, Belgium.
Reviewers:
(1) Matheus Poletto, University of Caxias do Sul, Brazil.
(2) Hajira Tahir, Chemistry, University of Karachi, Pakistan.
(3) Anonymous, Technical University of Kosice, Slovakia.
Complete Peer review History: http://sciencedomain.org/review-history/10449

Original Research Article

Received 8th May 2015
Accepted 14th July 2015
Published 9th August 2015

ABSTRACT

Undried coir cellulose was prepared by chlorite bleaching method and hydrolyzed by 50% sulphuric acid to obtain highly crystalline nanocellulose. The proximate analysis of the coir fibre such as; moisture, ash, crude fibre, protein and its mineral composition were investigated using the AOAC standard protocol. The effect of hydrolysis on coir cellulose morphology was investigated using X-ray powder diffraction (XRD), scanning electron microscopy (SEM), transmission electron microscopy (TEM), atomic force microscopy (AFM). SEM, TEM and AFM images revealed that the nanocellulose dispersion consists of individual nanocellulose whiskers of about 200 nm in length and 10-30 nm in width. This study showed that cellulose nanocrystals (CNC) will be appropriate templates for surface nanostructures particularly in applications aimed at incorporating bio-materials in materials fabrication.

**Corresponding author: E-mail: esyikhuoria@yahoo.com;*

Keywords: Coir; chlorite bleaching; nanocellulose; morphology.

1. INTRODUCTION

Cellulose is the most abundant biopolymer and one of nature's wonder. It forms the base reinforcement unit for the hierarchical structures in various plant species which gives them the unusual ability to provide high mechanical strength, a high strength-to-weight ratio, and high toughness [1,2]. Cellulose impact on man is an evidence that natural cellulose-based materials have found extensive use in the areas of engineering over thousands of years which was proven by the enormous worldwide industries in forest products. Unique properties such as biodegradability, low density, availability, low pricing and easily modifiable surface properties of the nature's wonder [3-5] provide potential opportunities to develop new materials on cellulosic fibre.

Decreasing the particle size of cellulose fibres in bulk wood cells to nanofibrils largely increases the properties of cellulose. Cellulose nanocrystals (CNC) typically have size dimensions of 5-20 nm in diameter and length varying from 25-3000 nm. The high aspect ratio of these crystals accompanied with the presence of pendant hydroxyl groups on its surface makes these crystals readily desirous in functionalized applications [6]. CNC can be obtained by a number techniques with acid hydrolysis being one of the most widely used techniques [7]. The choice of the method of isolation of CNC is particularly important as the dimensions of CNC depends on the starting material and also varies with processing conditions such as acid concentration, hydrolysis time, acid to fibre ratio, hydrolysis temperature as well as sonication time [7-10].

Previous work on CNC includes applications as a reinforcement for polymer matrices [8], surface functionalization of CNC has also been carried out with the aid of living radical polymerizations, incorporation of alkyne and azide groups, as well as epoxy and amine groups on the surface of CNC for applications in click chemistry, fluorescence labelling and graft polymerization on CNC [11-14]. Synthesis of layer-by- layer self-assembled multilayer films via modifications involving the use of cationic polyelectrolytes such as poly (amideamine) epichlorohydrin (PAE), and poly(allylamine hydrochloride) (PAH), have also been reported [15-17]. Furthermore, literature reports have been made on surface modification of CNC to form chiral nematic ordered CNC in toluene through the synthesis of a triblock copolymer based on xyloglucan oligosaccharides [18]. Several other applications involving surface modification of CNC have also been reported [8-10].

In this work, cellulose was isolated from coir fibre and was thereafter hydrolyzed via suphuric acid hydrolysis to nanocellulose with its morphology tailored for specialized applications. Also, the tailored morphology of the CNC obtained was investigated to ascertain its suitability for applications in templating of surface nanostructures.

2. EXPERIMENTAL SECTION

2.1 Materials and Methods

2.1.1 Materials

Sodium chlorite, Sulphuric acid, Acetic acid and NaOH (97%) were procured from Sigma Aldrich Inc. (USA). Ultrapure deionized water (18.2 MΩ.cm, 25°C), Merck Millipore (Germany) was used for preparing all solutions. All chemicals used were of AR (analytical reagent) grade and used as received. The coir was separated from its pits, which was freshly harvested from a plantation in Benin-City, Edo-State, Nigeria.

3. FRACTIONATION OF CELLULOSE FROM COIR FIBRE

3.1 Extraction of Waxes, Oils and Resins

A known amount of coir fibres (dried at 100°C for 24 h) was placed in a 500 ml Soxhlet apparatus and extracted over a mixture of toluene, acetone and ethanol in a ratio of 4:1:1 to remove waxes, oil and resin. This was left for 7 h and then, the coir was washed with warm water (45-50°C) to remove other forms of impurities and dried under vacuum oven (at 50°C for 24 h) for further characterization and fractionation of cellulose.

3.2 Delignification of Coir Fibre (Bleaching - Lignin Extraction to Produce Holocellulose)

3 g of coir fibre pulp was placed in 1.5 wt/vol % of sodium chlorite ($NaClO_2$) (pH <4). Glacial acetic acid was added in proportion to keep the pH below 4.0. The solution became bright yellow

with the samples floating. The reaction was kept at a temperature of 90°C for over 4 hours. This process was repeated twice until there was no further Cl used up, the solution became yellow and there was no increase in pH. The solution was washed several times over Buckner funnel until a neutral pH was reached. Holocellulose (α-cellulose and β-hemicellulose) was obtained by the gradual removal of lignin.

3.3 Degrading of Hemi-Cellulose

The holocellulose obtained from delignification of coir was treated with 17% NaOH solution. The sample was stirred for 45-60 minutes. No heat was required because the flask will get hot since the hemicellulose dissolving NaOH is exergonic. The cellulose obtained was washed with deionized water and the conductivity was checked repeatedly to ensure complete removal of NaOH. The undried cellulose obtained was stored at 4°C.

3.4 Nanocellulose (NC) Preparation by Acid Hydrolysis

CNC was prepared according to a previously reported procedure [19,20]. In a typical experiment, 3 g of cellulose were hydrolysed by 64% sulphuric acid. This hydrolysis was achieved by adding drop-wise amount of concentrated sulphuric acid to a known water/coir cellulose suspension in an ice bath to reach the desired concentration with vigorous stirring for 15 min. The suspension was heated to 45°C for 70 min after the complete addition of sulphuric acid and was centrifuged (Remy cooling centrifuge 12°C) with ultrapure deionized water (10 min, 12000 rpm) repeatedly until the supernatant became turbid after repeated cycles. The suspension obtained was placed in a 11 kDa MWCO dialysis membrane and dialyzed against ultrapure deionized water until a constant pH was attained after three days. The suspension was sonicated for 15 min and freeze dried. The resulting CNC was divided into two parts, one for freeze drying and other was diluted to a concentration of 0.5% w/w in deionized water for further characterization.

4. CHARACTERIZATION TECHNIQUES

4.1 X ray Diffraction Analysis

Powder X-ray diffraction studies were performed to determine the crystal structure of as-synthesized nanocellulose in an angle range of 5-45° on an X-ray diffractometer (Philip's X'pertPro) with Cu Kα radiation (λ = 0.154) employing an X'celerator detector and a monochromator at the diffraction beam side. The samples were used by employing a standard sample holder.

The crystallinity index (CI) was calculated using the intensity values of the diffraction peaks corresponding to the crystalline and amorphous regions, according to the Segal method [19]:

$$CI = \frac{I_{(002)} - I_{(am)}}{I_{(002)}} X100$$

where $I_{(002)}$ is the counter reading at peak intensity of 2θ angle close to 26° representing crystalline material and $I_{(am)}$ is the counter reading at peak intensity of 2θ angle close to 18° representing amorphous material in coir cellulosic fibre.

The crystallinity index was also evaluated by the method proposed by Hermans et al. [21,22]:

$$CI' = A_{cryst.}/A_{tot.}$$

where A_{cryst} denotes the total area of the crystalline peaks at (101), (10$\underline{1}$), (021), and (002) crystallographic planes and $A_{tot.}$ is the total area under the diffractograms.

Calculation of the order of orientation (O.I) was done using the equation [22]:

$$O.I = [1- (I_{am}/I_{tot})]$$

where I_{am} is the intensity of the diffraction peak corresponding to the amorphous region and I_{tot} denotes the maximum intensity of the diffraction pattern.

4.2 Scanning Electron Microscopy (SEM) Analysis

SEM analysis of samples were performed using Zesis EVO 18 cryo SEM with variable pressure working at 15−30 kV. The samples were prepared by drop casting method.

4.3 Transmission Electron Microscopy (TEM) Analysis

TEM analysis of the sample was performed in an FEI, TECNAIS Twin microscopy with an accelerating voltage of 100 kV. The sample was

drop casted on a 400 mesh copper grid and allowed to air dry.

4.4 Fourier Transform Infrared Spectroscopy Analysis

The coir samples (fibre and CNC) were dispersed in KBr matrix to form pellets by compression. FT-IR spectra were recorded on these films using a Perkin-Elmer spectrophotomer 1 in transmission mode with a resolution of 4 cm^{-1}. The spectra were obtained using 32 scans, in the range of 4000 cm^{-1} to 500 cm^{-1}.

4.5 Proximate/elemental Analysis

Proximate and elemental analyses were done using the AOAC standard methods [23]. A 210/211VGP atomic absorption spectrophotometer (AAS) was used for the elemental analysis of the coir samples after wet digestion using $HNO_3/HClO_4$ digestion mixture.

4.6 Atomic Force Microscopy (AFM)

AFM imaging of cellulose nano-fibres (CNCs) was performed with a 'Nanoscope V' scanning probe microscope (Digital Instruments). A few drops of the diluted nanocellulose suspension (0.001 wt %) were deposited onto freshly cleaved mica substrate and allowed to dry. Samples were scanned in air at ambient relative humidity and temperature in tapping mode.

5. RESULTS AND DISCUSSION

Table 1 summarizes the characteristics of the coir fibre. The results obtained from the proximate analysis study showed that the coir fibre had a high fibre content but was low in ash, crude fat and % protein contents. The moisture content was slightly lower than the value (9.8%) reported for coir by Abraham et al. [24].

Elemental analysis of the coir fibre revealed that it contained low or no trace amounts of heavy metals as seen in the Table 1b, there are however traces of elements such as calcium, manganese and iron. The yield of cellulose was 20%; the low cellulose content was attributed to the way the fibre was processed because reasonable amount of cellulose was lost during washing.

A comparison of the proximate composition obtained for coir to literature reports for other fibres revealed that the coir sample showed higher moisture, ash, fat and protein contents compared to flax fibres which had values of 8.0%, 1.0%, 1.5%, and 3.0% respectively [25]. The proximate composition reported for hemp fibres was however higher in moisture content (10.0%), but lower in ash, fat and protein contents with values of 0.7%, 0.7%, and 1.4% respectively [25].

Table 1a. Proximate composition of coir

Component	Content (%)
Moisture	9.50
Ash	3.20
Crude fat	10.20
Crude fibre	47.00
Crude protein	5.18
Nitrogen free extract	28.32

N.D = Not Detected

Table 1b. Elemental analysis of coir

Elements	Amount (ppm)
Calcium	2.40
Cadmium	N.D
Cobalt	8.00
Manganese	0.50
Iron	12.60
Lead	ND

The FT-IR spectra of coir fibre and the cellulose (a & b) are presented in Fig. 1. The spectra can be categorized into two regions: the region corresponding to O-H and and C-H stretching vibrations (3600-2700 cm^{-1}) and the 'fingerprint' region corresponding to the stretching vibrations exhibited by groups in the various components of wood (1800-600 cm^{-1}). The coir fibre exhibits the characteristic lignocellulosic absorption bands, which include a broad peak of the cellulose and lignin hydroxyl groups (O-H) at 3394 cm^{-1} while the CNC gave a corresponding peak due to cellulose hydroxyl groups at 3400 cm^{-1}. The peaks at 2933 cm^{-1} and 2904 cm^{-1} for coir and CNC respectively correspond to the C-H stretching vibrations of methyl and methylene groups.

The band at 1738 cm^{-1} corresponds to the stretching vibrations of C=O group present in carboxyl and acetyl groups of hemicellulose, the absence of this peak in the CNC spectra confirms the loss of hemicellulose in the synthetic procedure for CNC.

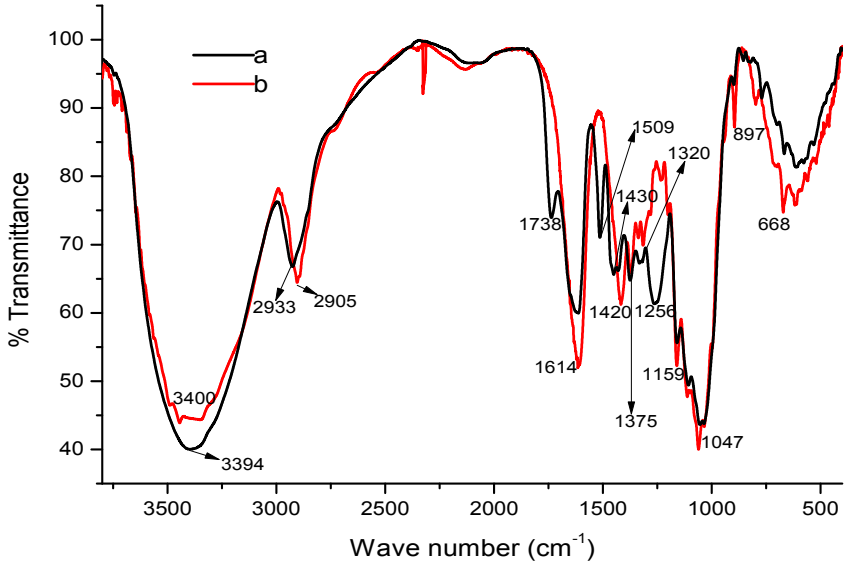

Fig. 1. Fourier transform infrared (FT-IR) spectra of the coir fibre (a) and the modified coir fibre (nanocellulose) (b)

The presence of bands at 1509 cm^{-1} and 1256 cm^{-1} (corresponding to vibrations of the C=C moiety in benzene ring and the guaiacyl/syringyl ring stretching vibrations respectively) in coir and their absence in CNC confirms the removal of lignin from coir to obtain the synthesized CNC.

Peaks at 1047 cm^{-1} and 1420 cm^{-1}, 1430 cm^{-1} correspond to deformation, bending and stretching vibrations of C-H, C-O in various groups in carbohydrates. Characteristic cellulose peaks corresponding to C-H deformations (897 cm^{-1}), C-O-C stretching vibrations (1159 cm^{-1}) were also observed. The peaks at 1614 cm^{-1} and 668 cm^{-1} can be assigned to OH bending due to absorbed water and C-OH out-of-plane bending in cellulose respectively [22,26-31].

The unique properties of cellulose such as its strength and crystallinity are largely due to intramolecular (O(2)H---O(6) and O(3)H---O(5) bonding) and intermolecular hydrogen bonding (O(6)H---O(3') bonding) facilitated by the presence of pendant hydroxyl groups in cellulose [30,31]. Hydrogen bonding is aided by high degree of orientation and low hydrogen bond distance in cellulose which increase the degree of packing of cellulose nanofibrils. The degree of hydrogen bonding is readily seen in the broadening of the band corresponding to O-H stretching; the extent of deviation of this band from the typical frequency of free O-H absorption is used to estimate the degree of hydrogen bonding in cellulose chains. This index is called the energy of hydrogen bonds [21,30,32].

The energy of hydrogen bonds (E_H) for CNC and coir was estimated using the equation [21,30]:

$$E_H = 1/k[(v_o - v)/ v_o]$$

where v_o is the frequency assigned to free hydroxyl groups (3650cm^{-1}), v is the observed frequency for the hydrogen bonded hydroxyl groups and k denotes a constant (1/k = 2.625 x10^2 kJ).

The hydrogen bond distance (R) was estimated using the Pimentel and Sederholm equation [21,30]:

$$\Delta v(cm^{-1}) = 4430 \times (2.84-R)$$

where $\Delta v(cm^{-1}) = (v_o - v)$ v_o is the monomeric OH stretching frequency with a value of 3600cm^{-1} and v is the observed frequency in the IR spectra.

The hydrogen bond distance (R) and the energy of hydrogen bond (E_H) obtained for coir (at 3394 cm^{-1}) and CNC (at 3400 cm^{-1}) were close to the values reported by Poletto et al. at IR

frequencies of 3423 cm^{-1} [21,32] and Popescu et al at IR frequencies of 3422 cm^{-1} [33] for cellulose in unprocessed wood fibres. The E_H value obtained for coir fibre was higher than the value for the synthesized CNC, while the hydrogen bond distance obtained was similar. However, considering the usually higher degree of orientation and crystallinity in CNC compared to cellulose in natural fibres [6] which was confirmed by XRD characterization in this study (Table 3), CNC should be expected to show a degree of hydrogen bonding higher than that in coir. The obtained result can be attributed to the fact that during the isolation of CNC from cellulose by sulphuric acid hydrolysis, some of the hydroxyl groups were esterified, resulting in disruption of the hydrogen bond network and hence a reduction in the energy of hydrogen bonding [28,34].

Analysis of the FT-IR spectra of cellulose has been reported as a means of estimating the degree of crystallinity and orientation in cellulose fibres, this is done following the method by Nelson and O'Connor [35,36] in which the ratio of certain bands corresponding to specific regions of cellulose is used as empirical indices to estimate the order in the cellulose chains [21,30, 32]. The method is based on the fact that the O-H and C-H stretching absorptions are dependent on the degree of order in the cellulose chains [31]. The band at 1420-1430 cm^{-1} corresponds to the amount of crystalline regions in the cellulose chains while the band at about 898 cm^{-1} corresponds to the amorphous region in the cellulose chains; the ratio of the absorptions of both bands was referred to as the lateral order index (LOI). The LOI index therefore corresponds to the relative abundance of crystalline and amorphous regions in the cellulose chains, broadening of bands at these frequencies (1420-1430 cm^{-1} and 898 cm^{-1}) also indicates more disordered structure [31]. Nelson and O'Connor [35,36] also assigned the ratio of absorption of the bands at about 1372 cm^{-1} and 2900 cm^{-1} as the total crystallinity index (TCI) which was proposed as a an index to estimate the infrared crystallinity (IR) ratio. Furthermore, hydrogen bond intensity (HBI), which is dependent on the mobility of the cellulose chains as well as their bond distance was used as an index to measure the degree of crystallinity, chain regularity as well as the extent to which water molecules are bound to the cellulose chains. This index was assigned to the band ratio of the absorption bands at about 3400 cm^{-1} and 1320 cm^{-1} [21,32]. The obtained LOI, TCI and HBI values for both coir and CNC were similar, but higher than the values reported for *Pinus elliottii*, *Eucalyptus grandis* , *Mezilaurus itauba*, and *Dipteryx odorata* [37].

The use LOI and TCI values in the elucidation of the crystallinity of cellulose samples has been reported as a very simplistic approach which gives only relative values, this is because the spectral bands always contain contributions from both the crystalline and amorphous regions [31].

The XRD pattern of the CNC is shown in Fig. 2. The pattern shows diffraction peaks at 2θ reflections = 15.0° corresponding to the (101) crystallographic plane, 16.5° corresponding to the (10$\underline{1}$) crystallographic plane, 18.0° corresponding to the amorphous region, 20.4° corresponding to the (021) crystallographic plane and 22.5° corresponding to the (002) crystallographic plane. Modification of the cellulose with sulphuric acid gave highly oriented crystallites as seen in the XRD parameters in Table 3. The crystallinity index (CI) obtained for the synthesized CNC was about 78.55% based on Segal's method.

Table 2. Parameters from FT-IR analysis of CNC (a) and coir (b)

(a)

FT-IR indices	E_H(kJ)	R(Å)	IR crystallinity ratio		HBI A3400/A1320
			LOI $H1420/H897$	TCI H1375/H2905	
Values	17.98	2.80	4.57	0.95	1.91

(b)

FT-IR indices	E_H(kJ)	R(Å)	IR crystallinity ratio		HBI A3394/A1320
			LOI $H1430/H897$	TCI H1375/H2933	
Values	18.41	2.79	5.10	1.06	1.84

Rezanezhad et al. [26] and Chen et al. [27] had earlier reported CI of (62.79%) and (63.40%) obtained for nanocellulose from rice and wheat straw respectively, which were lower than our reported values. The crystallinity index (CI') obtained by the Herman's method was 64.63%. A comparison of the crystallinity index obtained by the Segal's method and the Herman's method agrees with reports by Xu et al. [38], Polleto et al. [21, 37] and Popescu et al. [22], who also reported higher crystallinity index values by the Segal's method. However, the Segal's method has been reported as an inadequate method of estimating crystallinity index due to fact that its value is based on the (200) crystallographic plane, thereby neglecting the crystallographic planes at (101) and (101). It is still informative however, when its value is quoted relative to values obtained from other methods to aid comparative analysis [38]. Studies have also shown that the CNCs surfaces are negatively charged with sulfate groups which provide electrostatic repulsion amongst individual CNCs to form homogenous and stable aqueous suspensions [28]. This implied that the generation of CNCs by acid hydrolysis will result in reduction in the level of hydrogen bond formation which consequently affects the crystallinity of the highly ordered and closely packed crystallites of CNCs. The effect of this was observed in the slightly higher value of E_H for coir compared to that for the synthesized CNC despite the crystalline nature of the latter.

The degree of orientation in the synthesized CNC is expectedly higher than that obtained for natural fibres as seen in the comparison of the obtained O.I value with that for Eucalyptus wood (with an O.I value of 0.636) [22]. This agrees with reports by Moon et al [6] in which nanonization of cellulose in cellulosic fibres was reported as a means of improving their crystalline properties. The high crystallinity index obtained for the synthesized CNC, can therefore be attributed to the degree of hydrogen bonding and the close-packing of nanofibrils demonstrated by the low hydrogen bonding distance, coupled with the high orientation index in the obtained fibres. The degree of crystallinity and order obtained from the XRD analysis also agrees with the TCI, LOI, and HBI values obtained from FT-IR analysis.

Table 3. Parameters from XRD analysis of CNC

XRD indices	C.I (%)	C.I'%	O.I
Values	78.55	64.63	0.88

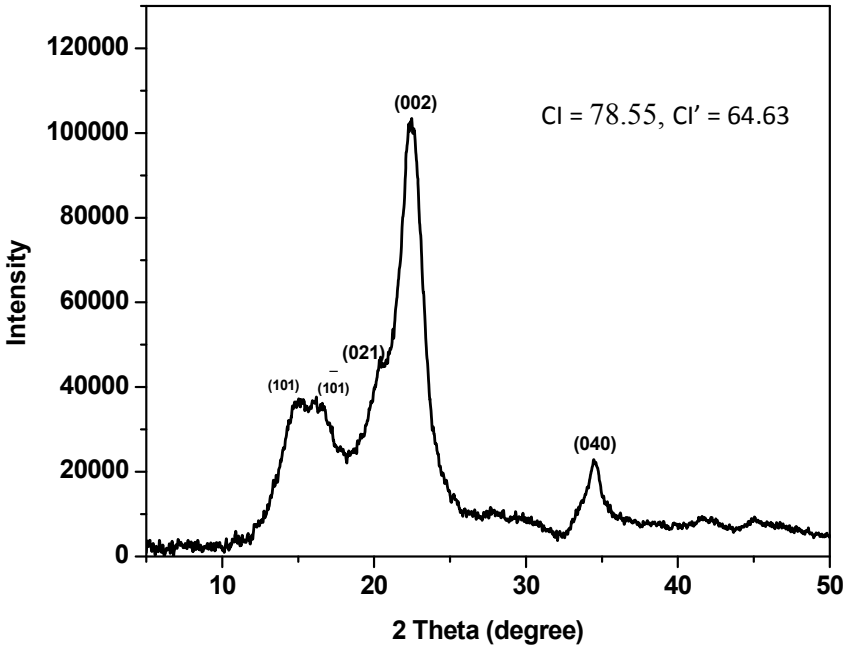

Fig. 2. XRD pattern of synthesized CNC

5.1 Morphological Properties

The diameter and morphology of the CNC template were studied by TEM, SEM and AFM imaging. Figs. 3 and 4 show the morphological assemblies of the CNC and its diameter which was between 10-30 nm with the length around 140 nm. This was consistent with other reports in literature [3,34,39].

As seen from the electron microscope images slight aggregation of the nanocellulose was observed and this could be attributed to the presence of hydrogen bonding in the cellulose nanofibre. The diameter of the CNC from this study is comparable with reported values for rice straw and soft wood with width and length of 5.5-6.6 nm and 58-515 nm [40,41], respectively reported on cellulose nano whiskers.

The TEM image shows a lower level of aggregation than the SEM micrograph. The results show that CNC particles are rod-like and can be considered as mono-dispersed.

The AFM phased image of the coir CNC obtained from the tapping mode manipulation showed the typical distribution of image data height under ambient conditions. The AFM image shows more regular particle size compared to Figs. 3 (a & b).

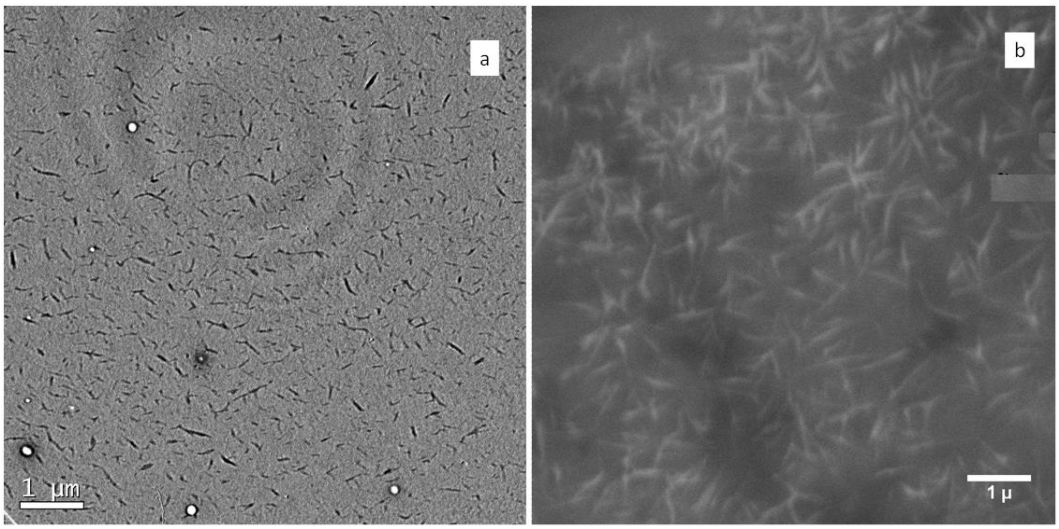

Fig. 3. TEM (a) and SEM (b) images of cellulose nanocrystals

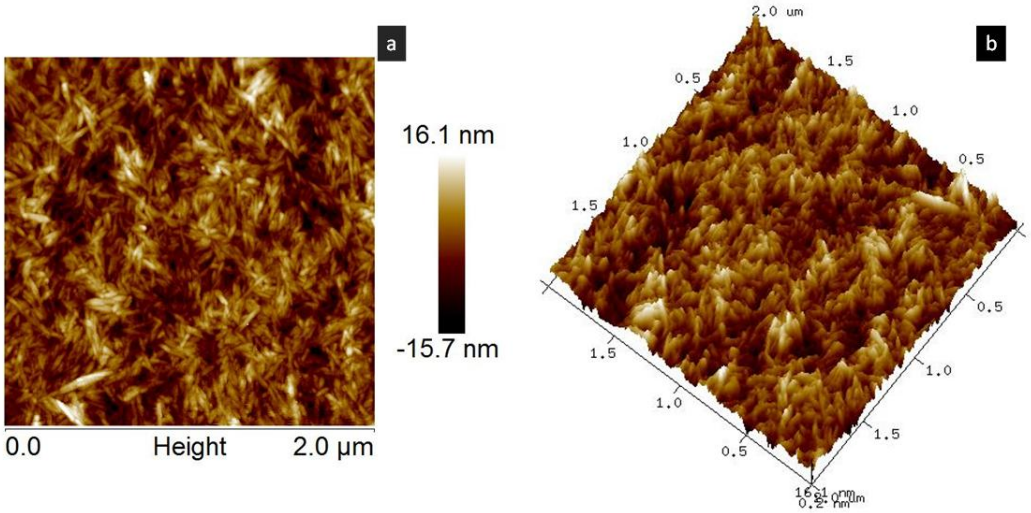

Fig. 4. Topography images (a) 2D and (b) 3D images obtained in tapping mode data

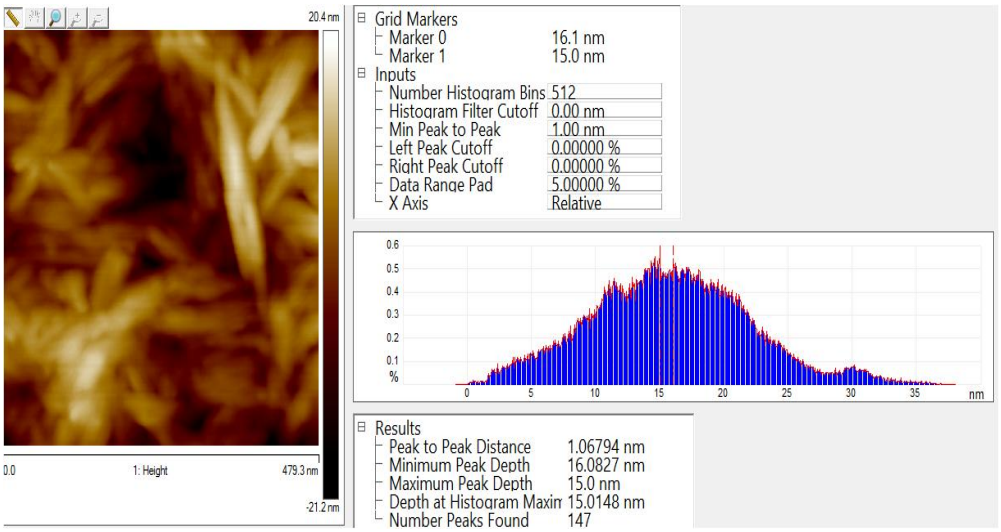

Fig. 5. AFM depth image obtained for CNC.

This was confirmed in Fig. 4b (3D image) which shows the surface roughness of the CNC. The processed AFM images show that the CNC height was between 5 to 30 nm as shown in the depth image in Fig. 5 above and the length was between 130 to 220 nm. The CNC height measurement was consistent, with slightly small changes within 1 nm run-to-run in the AFM height measurement. These slight changes in the height measurement could be linked with water molecules penetrating the CNC and diffusing between the particles and then causing a separation in the cellulose chains. This agrees with literature reports by Lahiji et al. [1] where humidity changes had no effect on the lattice spacing of cellulose determined by X-ray diffraction measurements. The size dimensions show that the CNC will be appropriate templates for surface nanostructures, particularly in applications aimed at incorporating bio-materials in materials fabrication.

6. CONCLUSION

This study showed that rice-shaped cellulose nanocrystals can be synthesized from coir fibres. The CNC particles were rod-like and can be considered as mono-dispersed particles. The characterization of the CNC showed high crystallinity, high aspect ratio and good surface properties which makes them appropriate for use as templates for surface nanostructures with potential application in the incorporation of bio-materials in materials fabrication.

ACKNOWLEDGEMENTS

M.R. Chandran and Soumya Valsalam are acknowledged for SEM acquisition and Kiran Mohan is acknowledged for TEM image acquisition. We thank Dr. Saju Pillai for fruitful discussions. This research was supported by TWAS-13-207RG/CHE/AF/AC_G-UNESCO FR; 3240277727

COMPETING INTERESTS

Authors have declared that no competing interests exist.

REFERENCES

1. Lahiji RR, Xu X, Reifenberger R, Raman A, Moon RJ. Atomic force microscopy of cellulose nanocrystals. Langmuir. 2010;26(6):4480-4488.
2. Padalkar S, Capadona JR, Rowan SJ, Weder C, Moon RJ, Stanciu LA. Self-assembly and alignment of semiconductor nanoparticles on cellulose nanocrystals. Journal of Material Science. 2011;46: 5672-5679.
3. Azizi Samir MAS, Alloin F, Dufresne A. Review of recent research into cellulosic whiskers, their properties and their application in nanocomposite field. Biomacromolecules. 2005;6(2):612-626.
4. Espert A, Vilaplana F, Karlsson S. Comparison of water absorption in natural cellulosic fibres from wood and one-year

crops in polypropylene composites and its influence on their mechanical properties. Composite. A-Applied Science and Manufacturing. 2004;35:1267-1276.
5. Pasquini D, Belgacem MN, Gandini A, Curvelo AAD. Surface esterification of cellulose fibers: Characterization by DRIFT and contact angle measurements. Journal of Colloid and Interface Science. 2006; 295:79-83.
6. Moon RJ, Martini A, Nairn J, Simonsen J, Youngblood J. Cellulose nanomaterials review: Structure, properties and nanocomposites. Chemical Society Reviews. 2011;40(7):3941-3994.
7. Beck-Candanedo S, Roman M, Gray DG, Mathew A. Effect of reaction conditions on the properties and behavior of wood cellulose nanocrystals suspensions. Biomacromolecules. 2005;6:1048-1054.
8. Bondeson D, Mathew A, Oksman K. Optimization of the isolation of nanocrystals from microcrystalline cellulose by acid hydrolysis. Cellulose. 2006;13:171-180.
9. Salajkova M, Berglund LA, Zhou Q. Hydrophobic cellulose nanocrystals modified with quartenary ammonium salt. Journal of Material Chemistry. 2012;22: 19798-19805.
10. Argyropoulos I, Filpponen I, Argyropolous DS. Regular linking of cellulose nanocrystals via click chemistry: Synthesis and formation of cellulose nanoplatelet gels. Biomacromolecules. 2010;11(4): 1060-1066.
11. Zoppe JO, Habibi Y, Rojas OJ, Venditti RA, Johansson LS, Efimenko K, Osterberg M, Laine J. Poly(N-isopropylacrylamide) brushes grafted from cellulose nanocrystals via surface-initiated single electron transfer living radical polymerizations. Biomacromolecules. 2010;11:2683-2691.
12. Xu QX, Zhang XF, Zhang HL. A novel amphotropic polymer based on cellulose Nanocrystals grafted with azo polymers. Eur. Polym. J. 2008;44:2830-2837.
13. Majoinen J, Walther A, McKee JR, Konturri E, Aseyev V, Malho JM, Ruokolainen J, Ikkala O. Polyelectrolyte brushes grafted from cellulose nanocrystals using Cu-mediated surface-initiated controlled radical polymerization. Biomacrmolecules. 2011;12(8):2997-3006.
14. Morandi G, Heath L, Thielemens W. Cellulose nanocrystals grafted with polystyrene chains through surface-initiated atom transfer radical polymerization (SI-ATRP). Langmuir. 2009; 25(14):8280-8286.
15. Ahola S, Osterberg M, Laine J. Cellulose nanofibrils-Adsorption with poly(amideamine)epichlorohydrin studied by QCM-D and application as a paper strength additive. Cellulose. 2008;15:303-314.
16. Aloulou F, Boufi S, Beneventi D. Adsorption of organic compounds onto polyelectrolyte Immobilized-surfactant aggregates on cellulosic fibres. Journal of Colloid and Interface Science. 2004; 280(2):350-358.
17. Cranston ED, Gray DG. Morphological and optical characterization of polyelectrolyte multilayers incorporating nanocrystalline cellulose. Biomacromolecules. 2006;7(9): 2522-2530.
18. Zhou Q, Brumer H, Teeri TT. Self-organization of cellulose nanocrystals adsorbed with xyloglucan oligosaccharide-poly(ethyleneglycol)-polystyrene triblock copolymer. Macromolecules. 2009;42: 5430-5432.
19. Favier V, Chanzy H, Cavaille JY. Polymer nanocomposites reinforced by cellulose whiskers. Macromolecules. 1995;28(18): 6365-6367.
20. Sèbe G, Ham-Pichvant F, Ibarboure E, Koffi ALC, Tingaut P. Supramolecular structure characterization of cellulose II nanowhiskers produced by acid hydrolysis of cellulose I substrates. Biomacromolecules. 2012;13(2):570-578.
21. Poletto M, Zattera AJ, Forte MMC, Santana RMC. Thermal decomposition of wood: influence of wood component and cellulose crystallite size. Bioresource Technology. Elsevier Limited. 2012;109: 148-153.
22. Popescu C-M, Popescu M-C, Singurel G, Vasile C, Argyropoulos DS, Willfor S. Spectral characterization of of *Eucalyptus* wood. Applied Spectroscopy. 2007;61: 1168-1177.
23. AOAC, Official Methods of Analysis of the Association of Official Analytical Chemists; 2003.
24. Abraham E, Deepa B, Pothen LA, Cintil J, Thomas S, John MJ, Anandjiwalad R, Narine SS. Environmental friendly method for the extraction of coir fibre and isolation of nanofibre. Carbohydrate Polymers. 2013;92:1477-1483.

25. Bismarck A, Aranberri-Askargorta I, Springer J, Lampke T, Wielage B, Stamboulis A, Shenderovich I, Limbach H-H. Surface characterization of flax, hemp and cellulose fibres; surface properties and the water uptake behavior. Polymer Composites. 2002;23(5):872-894.
26. Rezanezhad SNN, Asadpur G. Isolation of nanocellulose from rice waste via ultrasonication. Lignocellulose. 2013;2(1): 282-291.
27. Chen Y, Liu C, Chang PR, Cao X, Anderson DP. Biocomposites based on pea starch and cellulose nanowhiskers hydrolyzed from pea hull fibre: Effect of hydrolyssis time. Carbohydrate Polymers. 2009;76(4):607-615.
28. Jiang F, Esker AR, Roman M. Acid-catalyzed and solvolytic desulfation of H2SO4-hydrolyzed cellulose nanocrystals. Langmuir. 2010;26(23):17919-17925.
29. Popescu M-C, Popescu C-M, Lisa G, Sakata Y. Evaluation of morphological and chemical aspects of different wood species by spectroscopy and thermal methods. J. Mol. Struct. 2011;988:65-72.
30. Poletto M, Zattera AJ, Santana RMC, Structural differences between wood species: evidence from chemical composition, FTIR spectroscopy, and thermogravimetric analysis. Journal of Applied Polymer Science. 2012;120(5):7.
31. Mizi Fan DDaBH. Fourier transform infrared spectroscopy for natural fibres. In Fourier Transform - Materials Analysis, D.S. Salih, Editor. 2012;45-61.
32. Poletto M, Ornaghi Júnior HL, Zattera AJ, Native Cellulose: Structure, characterization and thermal properties. Materials. 2014;7:6105-6119.
33. Popescu C-M, Singurel G, Popescu M-C, Vasile C, Argyropoulos DS, Willfor S. Vibrational spectroscopy and X-ray diffraction methods to establish the differences between hardwood and softwood. Carbohydrate Polymers. 2009; 77:851-857.
34. Habibi Y, Lucia LA, Rojas OJ, Cellulose nanocrystals: Chemistry, self-assembly, and applications. Chemical Reviews. 2010; 110(6):3479-3500.
35. Nelson ML, O'Connor RT. Relation of certain infrared bands to cellulose crystallinity and crystal lattice type. Part 1. Spectra of lattice types I, II, III, and of amorphous cellulose. J. Appl. Polym. Sci. 1964;8:1311-1324.
36. Nelson ML, O'Connor RT. Relation of certain infrared bands to cellulose crystallinity and crystal lattice type. Part II. A new infrared ratio for estimation of crystallinity in cellulose I and II. J. Appl. Polym. Sci. 1964;8(3):1325-1341.
37. Poletto M, Zattera AJ, Santana RMC. Structural differences between wood species: evidence from chemical composition, FTIR spectroscopy, and thermogravimetric analysis. Journal of Applied Polymer Science. 2012;126:336-343.
38. Xu F, Shi Y-C, Wang D. X-ray scattering studies of lignocellulosic biomass: A review. Carbohydr. Polym. 2013;94:904-917.
39. Nainggolan H, Gea S, Bilotti E, Peijs T, Hutagalung SD. Mechanical and thermal properties of bacterial-cellulose-fibre-reinforced Mater-Bi(®) bionanocomposite. Beilstein Journal of Nanotechnology. 2013; 4:325-329.
40. Lu P, Hsieh HL. Preparation and characterization of cellulose nanocrystals from rice straw. Carbohydrate Polymers. 2012;87:564-573.
41. Rosa MF, Medeiros ES, Malmonge JA, Gregorski KS, Wood DF, Mattoso LHC, Glenn, G, Orts WJ, Imam SH. Cellulose nanowhiskers from coconut husk fibers: Effect of preparation conditions on their thermal and morphological behavior. Carbohydrate Polymers. 2010;81:83-92.

Peer-review history:
The peer review history for this paper can be accessed here:
http://sciencedomain.org/review-history/10449